SPANDIDOS PUBLICATIONS

MOLECULAR MEDICINE REPORTS 30: 172, 2024

The role and mechanism of action of miR-92a in endothelial cell autophagy

WEILI CAO, BOXIN ZHAO, LIN GUI, XUEYUAN SUN, ZHIYONG ZHANG and LIJUAN HUANG

Clinical Laboratory, The Second Affiliated Hospital of Harbin Medical University, Harbin, Heilongjiang 150081, P.R. China

Received March 7, 2024; Accepted June 17, 2024

DOI: 10.3892/mmr.2024.13296

Abstract. Although microRNAs (miRNAs/miRs) serve a significant role in the autophagy of vascular endothelial cells (ECs), the effect of miR-92a on the autophagy of ECs is currently unclear. Therefore, the present study aimed to investigate the impact of miR-92a on autophagy in ECs and the underlying molecular processes that control this biological activity. Firstly, an autophagy model of EA.hy926 cells was generated via treatment with the autophagy inducer rapamycin (rapa-EA.hy926 cells). The expression levels of miR-92a were then detected by reverse transcription-quantitative PCR, and the effect of miR-92a expression on the autophagic activity of rapa-EA.hy926 cells was studied by overexpressing or inhibiting miR-92a. The level of autophagy was evaluated by western blot analysis, immunofluorescence staining and transmission electron microscopy. Dual-luciferase reporter assays were used to confirm the interaction between miR-92a and FOXO3. The results demonstrated that the expression levels of miR-92a were decreased in the rapa-EA.hy926 cell autophagy model. Furthermore, overexpression and inhibition of miR-92a revealed that upregulation of miR-92a in these cells inhibited autophagy, whereas miR-92a knockdown promoted it. It was also confirmed that miR-92a directly bound to the 3'-untranslated region of the autophagy-related gene FOXO3 and reduced its expression. In conclusion, the present study suggested that miR-92a inhibits autophagy activity in EA.hy926 cells by targeting FOXO3.

Introduction

Cardiovascular disease is a significant hazard to human life and health. Research has established that the death of endothelial cells (ECs), inflammation, endothelial-to-mesenchymal transition, proliferation and migration, resulting from hypertension, hyperlipidemia, diabetes and smoking, serve crucial roles in the development of cardiovascular diseases (1). In addition, numerous studies (2,3) have shown that changes in the autophagic activity of ECs have important roles in the pathogenesis of cardiovascular diseases.

Autophagy is the process of encapsulating proteins and organelles to be degraded, and transporting them to lysosomes for degradation. Subsequently, the resulting amino acids, lipids, nucleic acids and carbohydrates are released into cells to support metabolic requirements (4). Under physiological conditions, when the nutrient supply is sufficient, the level of autophagy is very low, and a low level of basal autophagy is essential for cell survival; however, if the autophagy activity is inhibited to zero, the cells will die quickly (5). ECs are an important part of the vascular wall of the cardiovascular system. According to the time and degree of EC autophagy activation, the EC autophagy process serves a dual role in cardiovascular disease (3). Zhou *et al* (6) reported that resveratrol can protect human umbilical vein ECs (HUVECs) from palmitic acid-induced oxidative damage by inducing autophagy, thereby reducing endothelial oxidative damage in a transcription factor EB-dependent manner. Peng *et al* (7) demonstrated that the traditional Chinese medicine compound 13-methyl berberine (13-MB) may possess anti-atherosclerosis effects; 13-MB was shown to exert a protective role in a model of H_2O_2-induced cell injury by activating autophagy in HUVECs and inhibiting activation of the NLRP3 inflammasome. Zhang *et al* (8) reported that knockout of the RAGE gene reduced myocardial fibrosis by inhibiting excessive autophagy-mediated transformation of ECs into mesenchymal cells. Niu *et al* (9) revealed that metformin downregulated autophagy through the Hedgehog pathway, thereby reducing hyperglycemia-induced endothelial injury. Therefore, in cardiovascular diseases, autophagy may protect cells and clear damaged cell components; when cells are stimulated by stressors, such as nutrient deficiency, hypoxia and infection, autophagy can act to promote cell survival. However, conversely, excessive activation of autophagy can lead to excessive degradation of intracellular components, which in turn leads to cell death (10).

Notably, improving understanding of the effects of autophagy on the body and its potential for precise regulation is highly significant in the context of preventing or treating cardiovascular diseases. However, research has suggested that the mechanism of autophagy is complex and is regulated by

Correspondence to: Professor Lijuan Huang, Clinical Laboratory, The Second Affiliated Hospital of Harbin Medical University, 246 Xuefu Road, Nangang, Harbin, Heilongjiang 150081, P.R. China
E-mail: 1290793265@qq.com

Key words: microRNA-92a, EA.hy926 cells, autophagy, cardiovascular disease

a number of signaling pathways; among these, the regulation of autophagy by microRNAs (miRNAs/miRs) has become the focus of extensive research. miRNAs are small non-coding RNAs that negatively regulate gene expression by binding to the 3' untranslated region (3'-UTR) of different target mRNAs, thereby inducing mRNA degradation or inhibiting translation (11). Previous studies (12,13) have identified genetic factors leading to the onset of cardiovascular disease and have discussed the role of miRNAs in its pathogenesis. Among these, miR-92a is a member of the miR-17-92 family that has been reported to be related to the formation of vascular ECs (14-16). As a mechanosensitive miRNA closely related to cardiovascular diseases (17,18), miR-92a serves a significant role in regulating the dynamic equilibrium of vascular ECs. Several studies (19,20) have shown that miR-92a is associated with cardiovascular disease. In addition, clinical trials have demonstrated that miR-92a levels may be significantly increased in the serum of patients with cardiovascular diseases (21-25). Further receiver operating characteristic (ROC) analysis confirmed that miR-92a alone showed 85% sensitivity and 82.50% specificity for predicting cardiovascular diseases (26). The upregulation of miR-92a has a significant role in EC damage by inducing apoptosis, inflammation, endothelial-mesenchymal transition, oxidative stress, proliferation and migration; these processes contribute to the onset and progression of cardiovascular illnesses. Wu *et al* (17) revealed that the expression of miR-92a was elevated in the ECs of the aortic arch in mice and pigs that were subjected to disrupted blood flow; this increase in miR-92a led to heightened inflammation and permeability in the ECs by suppressing the expression of phosphatidic acid phosphatase type 2 B. Furthermore, Wiese *et al* (27) transfected miR-92a into human aortic ECs (HCAECs) and demonstration that overexpression of miR-92a directly regulated FAM220A to increase STAT3 phosphorylation, thereby promoting inflammatory responses to cholesterol and lipid accumulation in HCAECs. Shang *et al* (28) found that high expression of miR-92a promoted EC apoptosis and subsequent vascular inflammation by inhibiting the expression of the endothelial protective molecules Krüppel-like factor (KLF)2 and KLF4. However, whether miR-92a regulates the autophagic activity of EA.hy926 RECs by targeting the expression of FOXO3 has not been reported.

The present study aimed to examine the expression of miR-92a in a cell model of autophagy comprising EA.hy926 cells treated with the autophagy inducer rapamycin (rapa-EA.hy926 cells). Additionally, the study sought to elucidate the molecular mechanism via which miR-92a regulates autophagy in EA.hy926 cells.

Materials and methods

Cell culture and establishment of the autophagy model. EA.hy926 cells (Shanghai Zhongqiao Xinzhou Biotechnology Co., Ltd.) were cultured in Dulbecco's modified Eagle's medium (DMEM; Gibco; Thermo Fisher Scientific, Inc.) containing 10% fetal bovine serum (Biological Industries; Sartorius AG) and 1% streptomycin/penicillin (Beyotime Institute of Biotechnology) at 37˚C in a saturated humidity incubator containing 5% CO_2. When cell confluence reached 70-80%, the cells were starved in serum-free medium for 12 h to synchronize the cell cycle and were then incubated with rapamycin (cat. no. B20714; Shanghai Yuanye Biotechnology Co., Ltd.) at a concentration of 1,000 nM in a 5% CO_2 cell incubator at 37˚C for 6 h to establish the autophagy model. The cells in the control group did not receive any treatment.

Western blot analysis. LC3I/LC3II, p62, Beclin1 and FOXO3 expression levels were determined using western blotting. Total protein was extracted from EA.hy926 cells using radioimmunoprecipitation assay buffer (cat. no. P0013B; Beyotime Institute of Biotechnology) and were quantified using a BCA kit (cat. no. P0009; Beyotime Institute of Biotechnology). A Bio-Rad iMark microplate reader (Bio-Rad Laboratories, Inc.) was used to measure the absorbance value of each sample at a wavelength of 540 nm. The protein concentration was calculated according to the standard curve, after which, equal samples of protein (20 μg) were separated by SDS-PAGE on 10 or 20% gels, and were transferred to a polyvinylidene fluoride membrane. After being blocked with 5% skim milk for 1 h at room temperature, the membrane was incubated with rabbit primary antibodies against LC3I/LC3II (cat. no. WL01506; 16/14 kDa), p62 (cat. no. WL02385; 55 kDa), Beclin1 (cat. no. WL02508; 60 kDa) and FOXO3 (cat. no. WL02891; 70 kDa) (all from Shenyang Wanlei Biotechnology Co., Ltd. and diluted to 1:1,000) at 4˚C overnight. Subsequently, the membrane was incubated with a horseradish peroxidase-conjugated goat anti-rabbit IgG secondary antibody (cat. no. WLA023; 1:5,000, Shenyang Wanlei Biotechnology Co., Ltd.) at 37˚C for 1 h. Target bands were developed using a chemiluminescence substrate kit (cat. no. P0018S; Beyotime Institute of Biotechnology) and were analyzed using Image-Pro Plus software (version 6.0; Media Cybernetics, Inc.). β-actin (cat. no. WL0002d; 43 kDa; Shenyang Wanlei Biotechnology Co., Ltd.; diluted to 1:1,000) was used as an internal reference.

Immunofluorescence assay. Immunofluorescence analysis was performed to assess the expression of LC3B. The cells were fixed with 4% paraformaldehyde (cat. no. P0099; Beyotime Institute of Biotechnology) for 15 min at room temperature and permeabilized with 0.1% Triton X-100 (cat. no. P0096; Beyotime Institute of Biotechnology) for 15 min at room temperature. Goat serum (cat. no. C0265; Beyotime Institute of Biotechnology) was used to block the sections for 30 min at room temperature. Subsequently, the cells were incubated with an anti-LC3B rabbit antibody (cat. no. WL01506; 1:200; Shenyang Wanlei Biotechnology Co., Ltd.) at 4˚C overnight. The cells were then incubated with an AlexaFluor® 594-conjugated goat anti-rabbit IgG secondary antibody (cat. no. RS3611; 1:1,000; ImmunoWay Biotechnology Company) at room temperature for 1 h. The nuclei were stained at room temperature with DAPI (1 μg/ml; cat. no. C1006; Beyotime Institute of Biotechnology) for 10 min. A Leica TCS SP laser scanning confocal microscope (Leica Microsystem GmbH) was used to obtain micrographs. The immunofluorescence intensity was measured using Image-ProPlus 6.0 software (Media Cybernetics, Inc.).

Transmission electron microscopy (TEM). The treated cells were moved to a 1.5-ml centrifuge tube using a cell scraper and then centrifuged at 1,006.2 x g for 5 min at room temperature.

Subsequently, the supernatant was discarded, and 1 ml 2.5% glutaraldehyde (Beyotime Institute of Biotechnology) was added to the sediment for fixation at 4˚C for 4 h. The fixed samples were then washed with phosphate-buffered saline, dehydrated at 4˚C with successively increasing percentages of acetone (50, 70, 90 and 100%; 15 min each) and soaked overnight at room temperature with Spurr's resin. Subsequently, the samples were incubated overnight in a 37˚C oven and baked for 48 h in a 60˚C oven. The samples were then cut into ultrathin slices (60-80 nm) using an ultrathin microtome (Leica Microsystems GmbH), stained with uranyl acetate for 15 min at room temperature, rinsed with distilled water, stained with lead citrate for 15 min at room temperature, rinsed again with distilled water and observed by TEM (Hitachi, Ltd.) after air-drying overnight.

Reverse transcription-quantitative PCR (RT-qPCR). The expression levels of miR-92a and FOXO3 were measured using RT-qPCR. Briefly, total RNA was isolated from EA.hy926 cells using TRIzol® reagent (Invitrogen; Thermo Fisher Scientific, Inc.) according to the manufacturer's instructions. RNA was then reverse transcribed into cDNA using the Evo M-MLV Reverse Transcription Kit (cat. no. AG11705; Accurate Biotechnology Co., Ltd.) or the miRNA 1st strand cDNA synthesis kit (cat. no. AG11717; Accurate Biotechnology Co., Ltd.), according to the manufacturer's protocols, and qPCR reaction was carried out according to the following amplification conditions: Pre-denaturation at 94˚C for 2 min for one cycle; followed by 35 cycles of denaturation at 94˚C for 30 sec, annealing at 55˚C for 30 sec and extension at 72˚C for 2 min; and a final extension step at 72˚C for 6 min. The relative changes in mRNA expression were calculated using the $2^{-\Delta\Delta Cq}$ formula (29). Among them, the reverse miR-92a primer was obtained from its RT reagent kit (cat. no. AG11717; Accurate Biotechnology Co., Ltd.). GAPDH and U6 were used as internal controls for mRNA and miRNA, respectively, and the primers for qPCR were synthesized by General Biology (Anhui) Co., Ltd. with the following sequences: FOXO3, forward 5'-CTCTCTCGCCCATGCTCTAC-3', reverse 5'-CCGAGCCCTTGGTGGTATA-3'; miR-92a, forward 5'-TATTGCACTTGTCCCGGCCTG-3'; GAPDH, forward 5'-GGACCTGACCTGCCGTCTAG-3', reverse 5'-GAGGAGTGGGTGTCGCTGTT-3'; and U6, forward 5'-CTCGCTTCGGCAGCACA-3' and reverse 5'-CTCGCTTCACGAATTTGCGT-3'.

Cell transfection. Transfection of miR-92a mimics and inhibitor. miR-92a mimics, miR-92a inhibitor and their corresponding negative controls (NCs) were purchased from General Biosystems (Anhui) Corporation Ltd. Lipofectamine® 2000 (Invitrogen; Thermo Fisher Scientific, Inc.) was used for transfection according to the manufacturer's instructions. Briefly, the cells were uniformly inoculated into 6-well plates ($2x10^5$/well) and cultured at 37˚C and 5% CO_2 until the cell confluence reached 30-50% after 24 h. A miRNA storage solution was prepared at a final concentration of 20 μM by dissolving 2.5 μmol freeze-dried miRNA mimics, inhibitor, mimics NC and inhibitor NC in 125 μl deionized water. Subsequently, 10 μl miRNA storage solution was mixed with 240 μl serum-free DMEM; the final concentration of miRNA mimics and inhibitors was 100 nM. The miR-92a mimics, miR-92a inhibitor and their corresponding NCs were then transfected into cells using Lipofectamine 2000 at room temperature for 4-6 h. The subsequent experiments were conducted 48 h post-transfection.

The transfected cells were then cultured in conventional medium for 48-72 h. The sequences were as follows: miR-92a mimics, 5'-UAUUGCACUUGUCCCGGCCUGU-3'; miR-92a inhibitor, 5'-ACAGGCCGGGACAAGUGCAAUA-3'; miR-92a mimics NC, 5'-UUCUCCGAACGUGUCACGUTT-3'; miR-92a inhibitor NC, 5'-CAGUACUUUUGUGUAGUACAA-3'.

Small interfering RNA (siRNA) transfection. FOXO3 siRNA (siFOXO3) and NC siRNA (siFOXO3 NC) were acquired from General Biosystems (Anhui) Corporation Ltd. The cells were evenly seeded into 6-well plates ($2x10^5$/well) and incubated at 37˚C and 5% CO_2 until cell confluence reached 30-50% after 24 h. The cells were cultured with a mixture of siRNA and Lipofectamine 2000 in 100 μl serum-free DMEM, according to the manufacturer's instructions. The medium was replaced after 4-6 h, and the cells were cultured in a 5% CO_2 incubator at 37˚C for 48 h. The sequences were as follows: si FOXO3, sense 5'-AAAUAGCUACUUACCUUUGCAGU-3', antisense 5'-ACUGCAAAGGUAAGUAGCUAUUU-3'; and siFOXO3 NC, sense 5'-UGAAUUGUAAUACGACUCACUAU-3', antisense 5'-AUAGUGAGUCGUAUUACAAUUCA-3'.

Co-transfection of cells with miR-92a inhibitor + siFOXO3 and miR-92a inhibitor + siFOXO3 NC. A miRNA storage solution was prepared at a final concentration of 20 μM by dissolving 2.5 μmol freeze-dried miR-92a inhibitor in 125 μl deionized water. A total of 24 h before transfection, the cells were plated in 24-well cell culture plates in complete DMEM ($5x10^4$ cells/well). Cells were then transfected with 100 nM miR-92a inhibitor and 100 nM siFOXO3 or siFOXO3 NC for 4-6 h at room temperature using Lipofectamine 2000. Subsequent experiments were performed 72 h post-transfection.

Dual-luciferase reporter assay. The pmirGLO vector was synthesized by General Biology (Anhui) Co., Ltd. The potential target genes of miR-92a were predicted using StarBase (http://starbase.sysu.edu.cn/) database, which showed that the FOXO3 3'-UTR has a miR-92a-binding site. Logarithmic-phase cells were inoculated into 24-well plates at a density of $2x10^5$ cells/well. Subsequently, the cells were co-transfected with luciferase reporter vectors (FOXO3-WT, 5'-GTAAATTGTTGTGCAATTGTGG-3'; FOXO3-MUT, 5'-GTAAATTGTTGTATGATTGTGGTTA-3') and miR-92a mimics or NCs using Lipofectamine 2000. Luciferase activity was measured 24 h after transfection using a dual-luciferase reporter kit (Dual Luciferase Reporter Gene Assay Kit; Beyotime Institute of Biotechnology) and luciferase activity was normalized to *Renilla* luciferase activity.

Statistical analysis. Each experiment was conducted at least three times and data are presented as the mean ± standard deviation. GraphPad Prism (version 9.0; Dotmatics) was used for statistical analysis. Comparisons between two groups were performed using an unpaired Student's t-test (independent-samples t-test). Comparisons among multiple

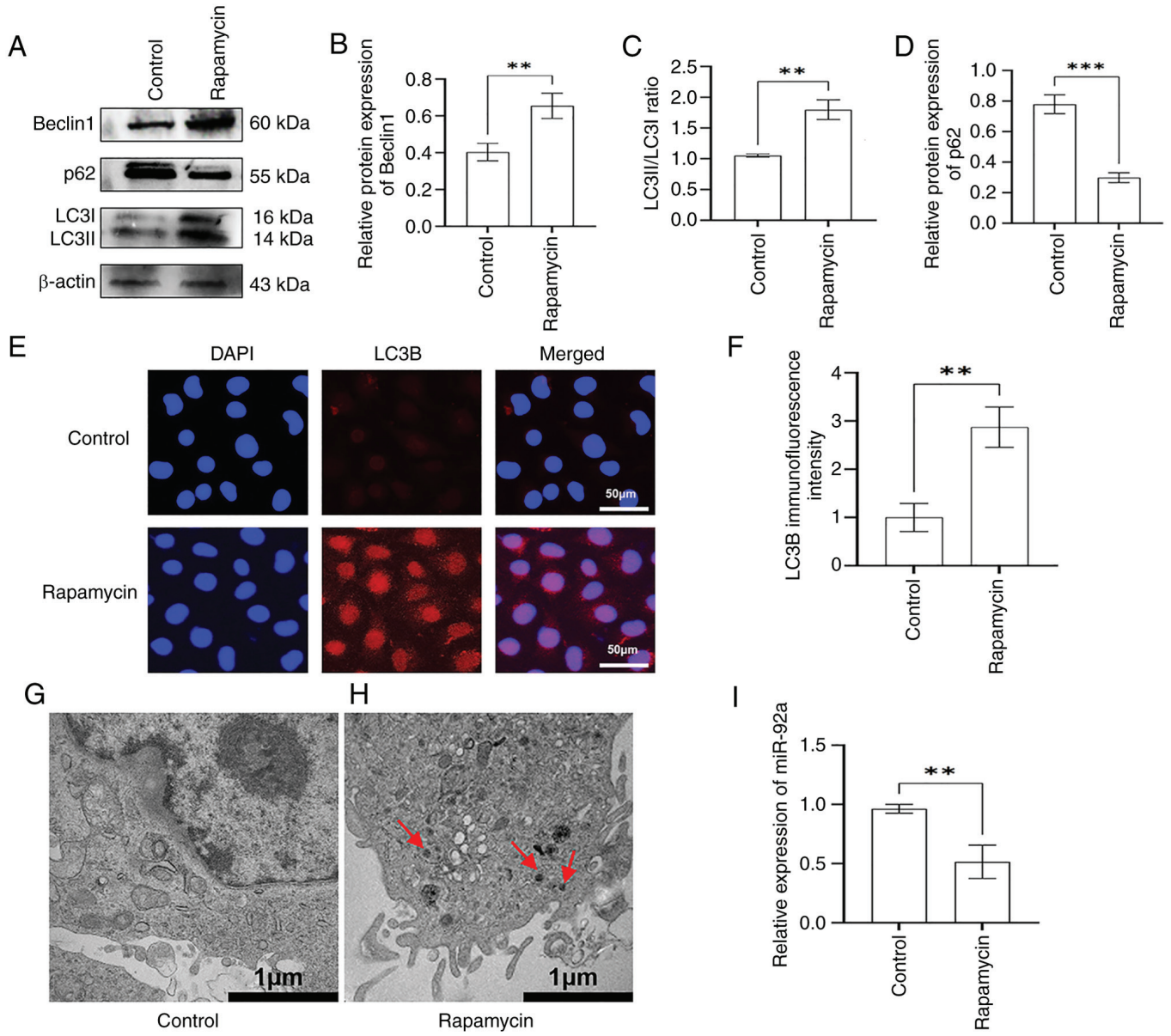

Figure 1. Effects of the autophagy inducer rapamycin on autophagy and miR-92a expression in EA.hy926 cells. (A) Western blotting was used to detect the expression levels of the autophagy-related proteins Beclin1, p62 and LC3II/I in EA.hy926 cells treated with rapamycin. Semi-quantitative analysis of western blotting showed that the (B) expression of Beclin1 and the (C) LC3II/I ratio were higher in EA.hy926 cells treated with rapamycin, whereas (D) p62 expression was lower. (E) Immunofluorescence assay was used to determine the immunofluorescence intensity of LC3B in EA.hy926 cells. Red, LC3B protein; blue, DAPI nuclear staining. (F) Semi-quantitative analysis of the immunofluorescence assay showed that the expression of LC3B was higher in EA.hy926 cells treated with rapamycin. Results of transmission electron microscopy showed that there was (G) no obvious autophagosome formation in EA.hy926 cells in the control group; however, (H) there were obvious autophagosomes in the rapamycin-treated EA.hy926 cells (red arrows indicate autophagosomes). (I) Reverse transcription-quantitative PCR results showed that the expression of miR-92a was lower in EA.hy926 cells treated with rapamycin. **P<0.01, ***P<0.001.

groups were performed with one-way ANOVA and Tukey's post hoc test. P<0.05 was considered to indicate a statistically significant difference.

Results

Rapamycin promotes EA.hy926 cell autophagy and inhibits the expression of miR-92a. Rapamycin, a strong and effective autophagy inducer, is known to stimulate ECs to undergo autophagy when incubated at a concentration of 1,000 nM for 6 h (30). In order to examine the association between miR-92a and autophagy in the EA.hy926 cell line, the cells were exposed to rapamycin at a dose of 1,000 nM for a 6 h to create an autophagy model in EA.hy926 cells. The results of western blotting showed that, compared with in the control group, the expression levels of autophagy-related Beclin1 and the LC3II/I ratio were significantly increased in the rapamycin group (Fig. 1A-C), whereas the expression levels of p62 were decreased (Fig. 1A and D). The results of immunofluorescence assay showed significantly increased fluorescence intensity of LC3B in the rapamycin group compared with that in the control group (Fig. 1E and F). TEM was used to count the number of autophagosomes in EA.hy926 cells in the control and rapamycin-treated groups. The results found that no obvious autophagosomes were present in the cytoplasm of the control group (Fig. 1G), whereas there was an increased number of autophagosomes in the cytoplasm of the rapamycin-treated group (Fig. 1H). These results indicated

that rapamycin activated autophagy in EA.hy926 cells, and the rapa-EC.hy926 autophagy model was established successfully.

To assess the association between miR-92a and autophagy in ECs, RT-qPCR was performed to detect the expression levels of miR-92a in the rapa-EA.hy926 cell autophagy model. The findings demonstrated a significant decrease in the expression of miR-92a in the rapamycin group compared with that in the control group (Fig. 1I). These findings indicated that miR-92a was abnormally expressed in the rapa-EA.hy926 autophagy model, suggesting that miR-92a may be involved in autophagy in this model system.

miR-92a regulates the autophagy function of rapa-EA.hy926 cells. To assess the impact of miR-92a on autophagy in EA.hy926 cells, miR-92a mimics or a miR-92a inhibitor were introduced into rapa-EA.hy926 cells using Lipofectamine. This allowed for the increase or decrease in the levels of miR-92a, hence creating experimental variations in miR-92a expression. The results of RT-qPCR indicated that the miR-92a mimics group exhibited a significant increase in the expression levels of miR-92a, indicating overexpression, compared with those in the mimics NC control group (Fig. 2A). Conversely, the miR-92a inhibitor group showed a significant decrease in the expression level of miR-92a, indicating inhibition. Western blot analysis demonstrated that, compared with those in the control group, the expression levels of Beclin1 and the LC3II/LC3I ratio in the miR-92a mimics group were decreased, and the protein expression levels of p62 were increased (Fig. 2B-E). By contrast, the expression levels of Beclin1 and the LC3II/LC3I ratio were higher in the miR-92a inhibitor group than those in the control group, whereas the protein expression levels of p62 were decreased. In addition, immunofluorescence staining results showed that the fluorescence intensity of LC3B in the miR-92a mimics group was significantly decreased compared with that in the control group, whereas the fluorescence intensity of LC3B in the miR-92a inhibitor group was increased compared with that in the control group (Fig. 2F and G). These findings indicated that the autophagy marker protein LC3B accumulated in the cytoplasm of the miR-92a inhibitor group. Furthermore, as number of autophagosomes were observed by TEM in the cytoplasm of the miR-92a inhibitor group, whereas no autophagosomes were apparent in the miR-92a mimics group, and only a small number of autophagosomes were observed in the miR-92a inhibitor and miR-92a mimic NC groups (Fig. 2H-K). These results suggested that overexpression of miR-92a may inhibit autophagy, whereas inhibition of miR-92a could enhance autophagy in rapa-EA.hy926 cells.

miR-92a directly binds to the FOXO3 3'-UTR region and negatively regulates FOXO3 expression. According to reports (31,32), miRNAs control several biological processes of cells by suppressing the transcription or translation of specific target genes at the post-transcriptional stage. Therefore, whether miR-92a is involved in the regulation of autophagy in EA.hy926 cells by acting on downstream target genes was explored. The bioinformatics software StarBase was used to analyze the downstream target genes of miR-92a. The results showed a binding site for miR-92a in the 3'-UTR region of FOXO3 (Fig. 3A); therefore, it was hypothesized that FOXO3 is a target gene for miR-92a. To assess this, FOXO3 wild-type and mutant luciferase reporter plasmids were constructed (Fig. 3B). Notably, luciferase activity in the miR-92a mimics + wild-type FOXO3 plasmid group was significantly lower than that in the miR-92a mimic NC + wild-type FOXO3 plasmid group (Fig. 3D). There was no significant difference in luciferase activity between the miR-92a mimic + mutant FOXO3 plasmid group and the miR-92a mimic NC + mutant FOXO3 plasmid group, which further confirmed that miR-92a directly binds to FOXO3 3'-UTR.

Subsequently, the impact of miR-92a on the control of FOXO3 gene expression was investigated. Western blotting and RT-qPCR showed that FOXO3 mRNA and protein expression levels were inhibited in the miR-92a mimics group compared with those in the control group, whereas FOXO3 mRNA and protein expression levels were enhanced in the miR-92a inhibitor group (Fig. 3C, E and F). In addition, FOXO3 mRNA and protein expression levels were significantly downregulated in the miR-92a mimics group compared with those in the miR-92a inhibitor group. These results indicated that the overexpression or inhibition of miR-92a can affect the expression of FOXO3 mRNA and protein. In summary, these findings suggested that FOXO3 may be a direct target of miR-92a in EA.hy926 cells and that miR-92a directly binds to a specific site on the FOXO3 3'-UTR to regulate its expression.

FOXO3 gene knockdown inhibits the autophagic activity of rapa-EA.hy926 cells. The present study demonstrated that miR-92a serves a role in controlling autophagy in EA.hy926 cells and that FOXO3 is a gene targeted by miR-92a. In addition, previous research (33) has indicated that FOXO3 has a significant role as an autophagic protein. Therefore, it was hypothesized that miR-92a might regulate the autophagy of EA.hy926 cells through FOXO3. To assess this hypothesis, the present study first investigated whether FOXO3 affected autophagy in EA.hy926 cells. siFOXO3 was transfected into cells using Lipofectamine to silence FOXO3. RT-qPCR and western blot analysis showed that FOXO3 mRNA and protein expression levels were significantly inhibited in the in siFOXO3 group of rapa-EA.hy926 cells compared with in the siFOXO3 NC group (Fig. 4A-C), indicating that FOXO3 siRNA was successfully transfected into cells. Western blotting was used to detect the expression levels of autophagy-related proteins in siFOXO3 cells. The results showed that, compared with in the siFOXO3 NC group, siFOXO3 transfection significantly decreased the expression levels of Beclin1 and the LC3II/I ratio, whereas p62 protein expression levels were increased (Fig. 4A and D-F). In addition, the immunofluorescence intensity of LC3B in siFOXO3 cells was weaker than that in the siFOXO3 NC cells (Fig. 4G and H). Furthermore, TEM revealed that autophagosomes were readily apparent in the siFOXO3 NC group, whereas no autophagosome formation was observed in the siFOXO3 group (Fig. 4I and J). Therefore, it was suggested that FOXO3 gene silencing inhibited autophagy in rapa-EA.hy926 cells.

siFOXO3 partially reversed the promoting effect of miR-92a inhibitors on rapa-EA.hy926 cell autophagy. To evaluate the role of miR-92a in regulating autophagy in EA.hy926

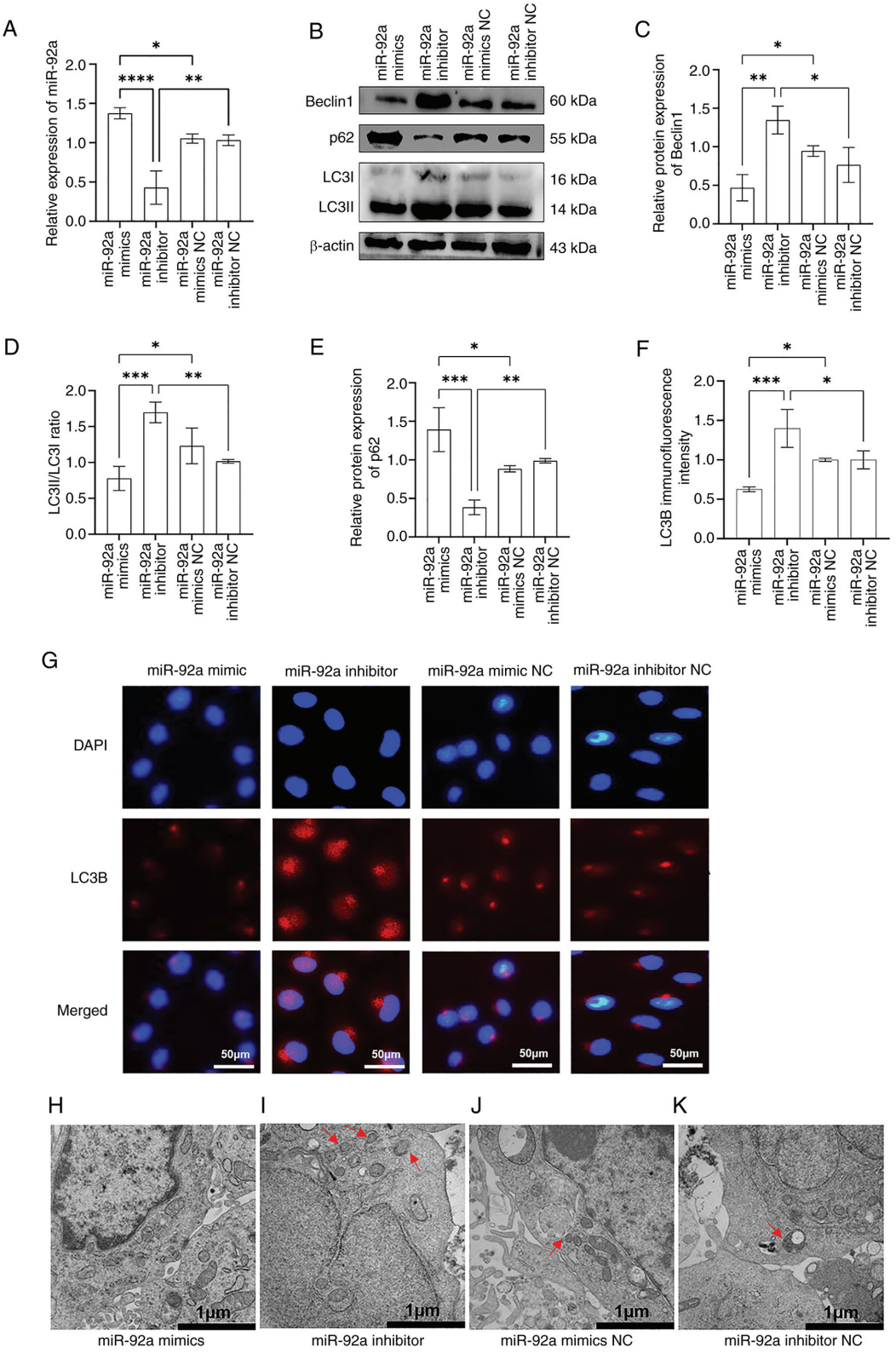

Figure 2. miR-92a inhibits the autophagic activity of rapamycin-treated EA.hy926 cells. (A) Reverse transcription-quantitative PCR results showed that after 48 h of transfection of rapamycin-treated EA.hy926 cells with miR-92a mimics, miR-92a inhibitor or corresponding NCs, the expression of miR-92a was upregulated in the miR-92a mimics group, whereas it was downregulated in the miR-92a inhibitor group, indicating that miR-92a mimics or inhibitors were successfully transfected into the cells. (B) Western blotting was used to detect the expression levels of autophagy-related proteins Beclin1, p62 and LC3II/I in the miR-92a mimics, miR-92a inhibitor or corresponding NC groups. Semi-quantitative analysis of western blotting showed that the (C) expression of Beclin1 and the (D) LC3II/I ratio were decreased in the miR-92a mimics group and were increased in the miR-92a inhibitor group, whereas (E) p62 was increased in the miR-92a mimics group and decreased in the miR-92a inhibitor group. (F) Results of LC3B immunofluorescence semi-quantitative analysis showed that the expression of LC3B in the miR-92a mimics group was decreased, whereas it was increased in the miR-92a inhibitor group. (G) Immunofluorescence assay was used to detect the immunofluorescence intensity of LC3B in the miR-92a mimics, miR-92a inhibitor or corresponding NC groups. Red, LC3B protein; blue, DAPI nuclear staining. Results of transmission electron microscopy in the (H) miR-92a mimics group, (I) miR-92a inhibitor group, (J) miR-92a mimics NC group and (K) miR-92a inhibitor NC group (red arrows indicate autophagosomes). *P<0.05, **P<0.01, ***P<0.001, ****P<0.0001. miR, microRNA; NC, negative control.

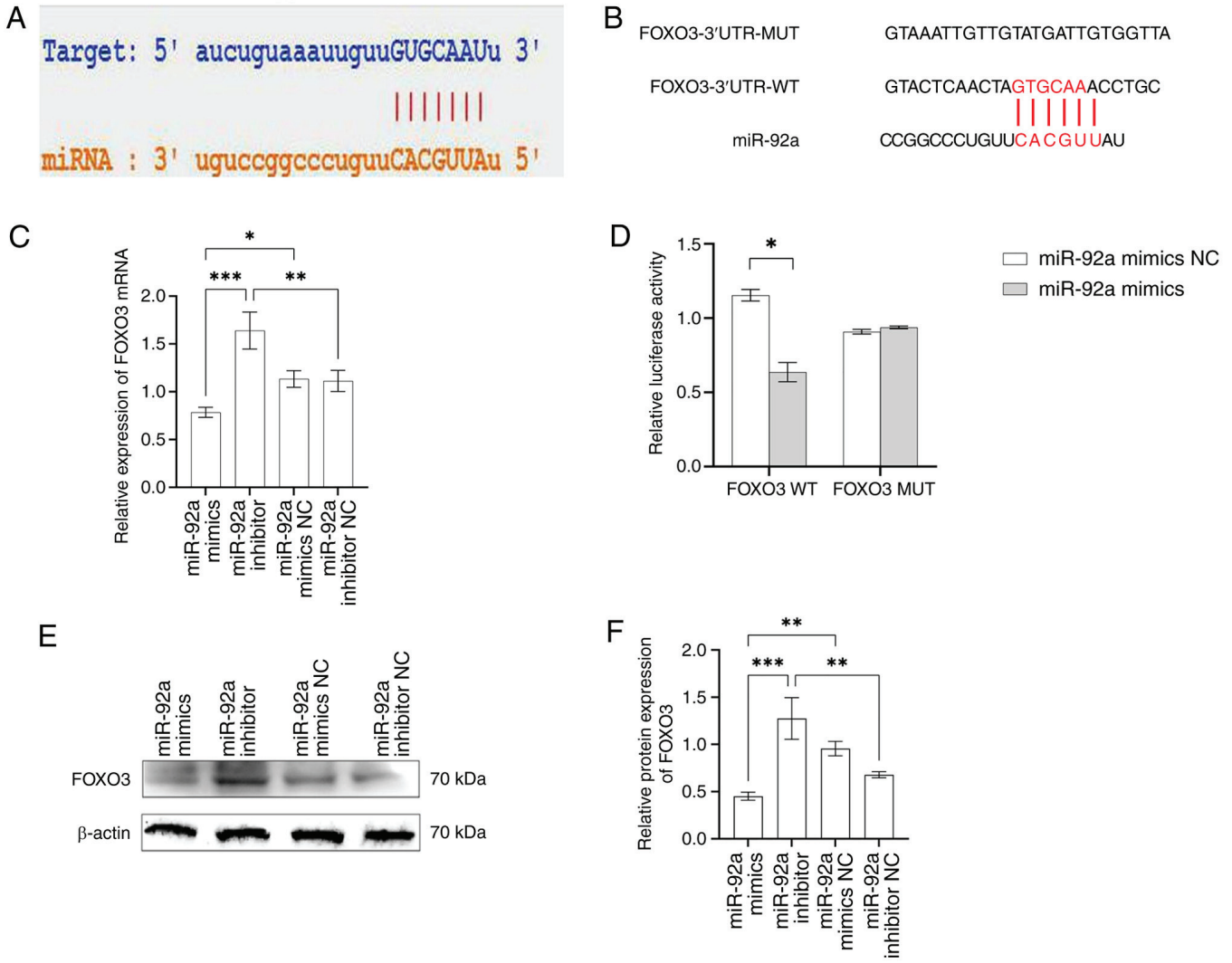

Figure 3. miR-92a inhibits FOXO3 protein and mRNA expression in EA.hy926 cells. (A) Binding site for miR-92a in the 3'-untranslated region of FOXO3. (B) Construction of FOXO3 WT and MUT luciferase reporter plasmids. (C) Reverse transcription-quantitative PCR was used to detect FOXO3 mRNA expression levels in rapamycin-treated EA.hy926 cells transfected with miR-92a mimics, a miR-92a inhibitor or corresponding NCs after 48 h. (D) A dual-luciferase assay confirmed the targeting relationship between miR-92a and FOXO3. (E) Western blotting of FOXO3 protein expression in rapamcyin-treated EA.hy926 cells transfected with miR-92a mimics, a miR-92a inhibitor or corresponding NCs, as determined by western blotting after 48 h. (F) Semi-quantification of the protein expression levels of FOXO3. *P<0.05, **P<0.01, ***P<0.001. miR, microRNA; MUT, mutant; NC, negative control; WT, wild-type.

cells via the suppression of FOXO3 expression, the rapa-EA.hy926 cells were transfected with miR-92a inhibitor + siFOXO3 or miR-92a inhibitor + siFOXO3 NC. Western blotting results showed that the expression levels of Beclin1 and the LC3II/I ratio in the miR-92a inhibitor + siFOXO3 group were decreased compared with those in the miR-92a inhibitor + siFOXO3 NC group, whereas the expression levels of p62 showed an opposite trend (Fig. 5A-D). Immunofluorescence results also showed that the fluorescence intensity of LC3B in the miR-92a inhibitor + siFOXO3 group was significantly weaker than that in the miR-92a inhibitor + siFOXO3 NC group (Fig. 5E and F). Similarly, only a few autophagosomes were detected in the cells of the miR-92a inhibitor + siFOXO3 group by TEM (Fig. 5 G and H). In conclusion, the results of siFOXO3 and miR-92a inhibitor co-transfection suggested that siFOXO3 can partially reverse the promoting effect of the miR-92a inhibitor on the autophagic activity of rapa-EA.hy926 cells. This further verified that miR-92a regulates autophagy in EA.hy926 cells by targeting FOXO3.

Discussion

Studies have confirmed that rapamycin is an autophagy inducer, and it is commonly used in the construction of various cell models of autophagy (34-36). To assess the association between miR-92a and autophagy in ECs, the stable human endothelial cell line EA.hy926 was subjected to treatment with rapamycin (1,000 nM) for 6 h to develop the rapa-EA.hy926 cell autophagy model. Rapa-EA.hy926 cells had increased Beclin1 protein expression, an increased LC3II/I ratio, decreased p62 expression, significantly increased LC3B immunofluorescence intensity, and increased formation of autophagosomes, as detected by TEM, compared with the control cells, suggesting that the rapa-EA.hy926 cell autophagy model was successfully constructed. This result is consistent with a previous report that ECs incubated with 1,000 nM rapamycin for 6 h exhibited a readily apparent increase in autophagy (30). The results of RT-qPCR showed significant downregulation of miR-92a in the EA.hy926

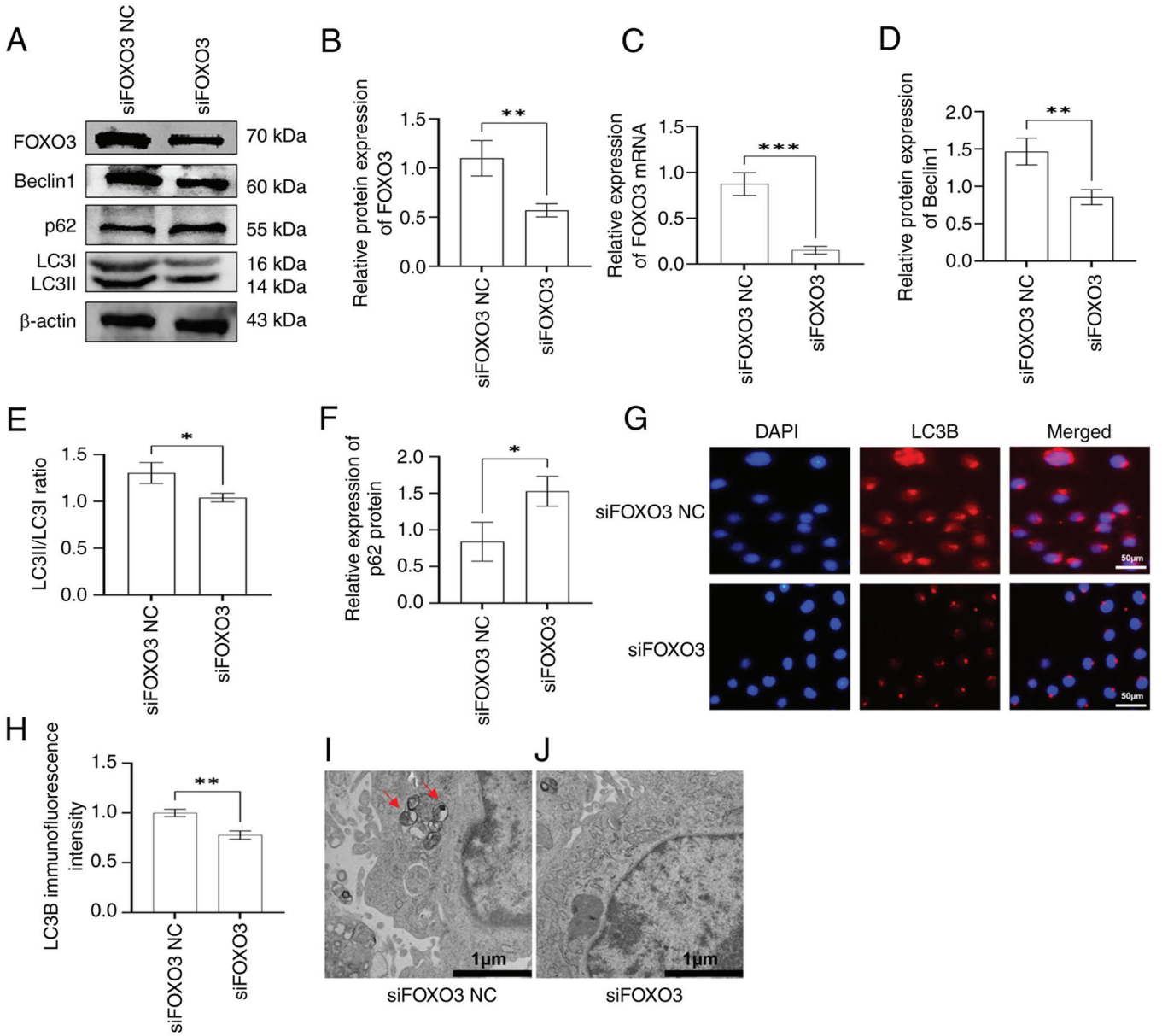

Figure 4. siFOXO3 inhibits the autophagic activity of rapa-EA.hy926 cells. (A) Western blotting was used to detect the expression levels of autophagy-related proteins Beclin1, p62, LC3II/I and FOXO3 in EA.hy926 cells in the siFOXO3 and siFOXO3 NC groups. (B) Semi-quantitative analysis showed that the expression of FOXO3 was downregulated in EA.hy926 cells in the siFOXO3 group, indicating that FOXO3 was successfully inhibited. (C) Reverse transcription-quantitative PCR results showed that the mRNA expression levels of FOXO3 were lower in the siFOXO3 group, indicating that FOXO3 was successfully inhibited. Semi-quantitative analysis of western blotting showed that (D) Beclin1 expression and the (E) LC3II/I ratio were lower in the siFOXO3 group, whereas (F) p62 expression was increased in the siFOXO3 group. (G) Immunofluorescence assay was used to determine the immunofluorescence intensity of LC3B in siFOXO3 and siFOXO3 NC groups. Red, LC3B protein expression; blue, DAPI nuclear staining. (H) Immunofluorescence semi-quantitative analysis of LC3B showed that the expression of LC3B was lower in the siFOXO3 group. Results of transmission electron microscopy showed that there were (I) obvious autophagosomes in the siFOXO3 NC group and (J) no obvious autophagosome formation in the siFOXO3 group (red arrows indicate autophagosomes). *P<0.05, **P<0.01, ***P<0.001. NC, negative control; si, small interfering.

cell autophagy model, suggesting a role for miR-92a in the regulation of EA.hy926 cell autophagy. To further determine the effects of miR-92a overexpression and knockdown on the autophagic activity of EA.hy926 cells, rapa-EA.hy926 cells were transfected with miR-92a mimics or a miR-92a inhibitor. The results indicated that miR-92a overexpression could inhibit the autophagic activity of rapa-EA.hy926 cells, whereas miR-92a knockdown enhanced the autophagic activity of rapa-EA.hy926 cells. These experimental results suggested that inhibition of EC autophagy by miR-92a may be another miR-92a-related cause of endothelial dysfunction. However, the mechanism by which miR-92a inhibits the autophagic activity of EC has not yet been reported.

Research (33) has demonstrated that miRNAs attach themselves to the 3'-UTR region of downstream target genes to control and influence cellular functions. In addition, has been suggested that miRNAs have a novel function in controlling EC autophagy (37). For example, miR-103 has been shown to protect coronary ECs from H_2O_2-induced oxidative stress damage through BNIP3-mediated end-stage autophagy (38), whereas miR-130a targets the expression of Runx3 to maintain the normal autophagy levels of endothelial progenitor cells

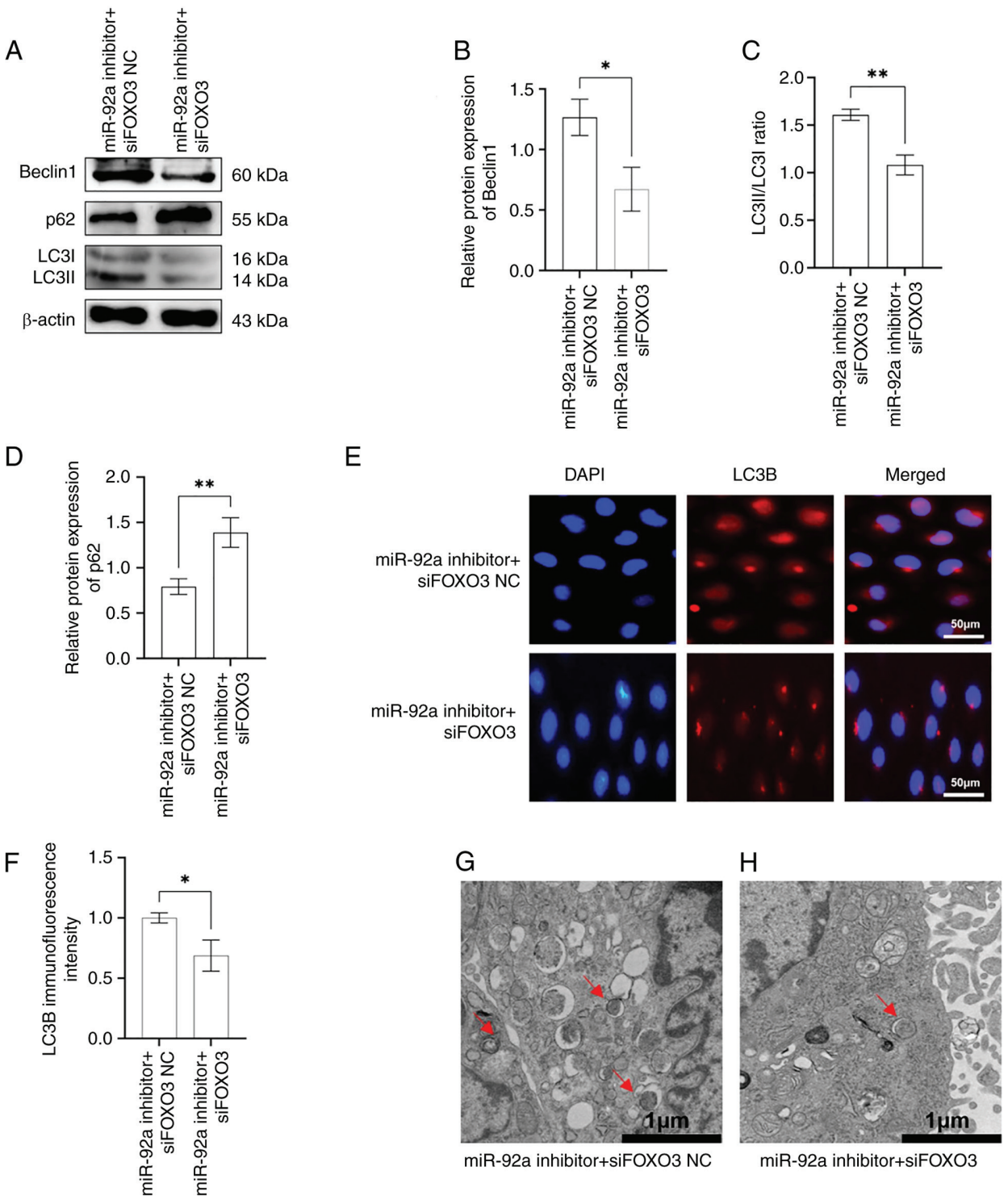

Figure 5. siFOXO3 partially reverses the enhancing effect of a miR-92a inhibitor on autophagy in rapamycin-treated EA.hy926 cells. (A) Western blotting was used to detect the expression levels of autophagy-related proteins Beclin1, p62 and LC3II/I in miR-92a inhibitor + siFOXO3 and miR-92a inhibitor + siFOXO3 groups. Semi-quantitative analysis of western blotting showed that the (B) expression of Beclin1 and (C) LC3II/I ratio were downregulated in the miR-92a inhibitor + siFOXO3 group, whereas (D) p62 expression was upregulated. (E) Immunofluorescence intensity of LC3B in the miR-92a inhibitor + siFOXO3 NC and miR-92a inhibitor + siFOXO3 groups was determined using an immunofluorescence assay. Red, LC3B expression; blue, DAPI nuclear staining. (F) Immunofluorescence semi-quantitative analysis of LC3B showed that the expression of LC3B was lower in the miR-92a inhibitor + siFOXO3 group. Results of transmission electron microscopy showed that there were (G and H) obvious autophagosomes in the miR-92a inhibitor + siFOXO3 NC group, whereas less autophagosome formation was detected in the miR-92a inhibitor + siFOXO3 group (red arrows indicate autophagosomes). *P<0.05, **P<0.01. miR, microRNA; NC, negative control; si, small interfering.

and promote their survival (39). Lu *et al* (40) proposed that propofol treatment could induce the expression of miR-30b, thereby alleviating hypoxia and reoxygenation-induced HUVEC damage, and upregulated miR-30b was shown to regulate HUVEC autophagic activity by targeting the expression of Beclin1.

To further analyze the mechanism by which miR-92a inhibits EC autophagy, the present study used bioinformatics software to screen and predict the target genes of miR-92a, and revealed that FOXO3 was a potential downstream target gene of miR-92a, which was confirmed by subsequent dual-luciferase experiments. Western blotting and RT-qPCR analysis showed that miR-92a mimics suppressed FOXO3 mRNA and protein expression, whereas the miR-92a inhibitor promoted FOXO3 mRNA and protein expression. Therefore, these results confirmed FOXO3 to be a target gene of miR-92a, and miR-92a may inhibit FOXO3 protein and mRNA expression by binding to its 3'-UTR region.

FOXO3 is a transcription factor that has a role in regulating several cellular activities. Previous studies have has demonstrated that FOXO3 functions as a tumor suppressor by controlling the expression of genes involved in apoptosis, cell cycle arrest and resistance to oxidative stress (41,42). In addition, numerous studies have shown that FOXO3 is associated with longevity and autophagy by directly activating the expression of autophagy-related proteins, thereby complementing core components of autophagy (43-46). In addition, it has been reported that FOXO3 is negatively regulated by miRNAs and participates in the process of autophagy. Li *et al* (47) reported that the expression of miR-221 was increased and the levels of FOXO3 were decreased in a rat model of myocardial infarction after myocardial fibrosis. By contrast, inhibition of miR-221 expression could inhibit the autophagic activity of cardiomyocytes, and the results of a luciferase reporter gene assay confirmed that FOXO3 was its downstream target gene. In addition, Song *et al* (48) proposed that miR-34a can inhibit autophagy of alveolar type II epithelial cells in acute lung injury by inhibiting FOXO3 expression, and FOXO3 was identified as a downstream target gene of miR-34a. Long *et al* (49) showed that miR-223-3p can regulate autophagy by acting on its target gene FOXO3, thus participating in the osteogenic differentiation of bone marrow mesenchymal stem cells. In summary, FOXO3 is known to serve a significant role in the process of autophagy as a target gene of miRNAs.

The present study validated that the excessive production of miR-92a can impede the process of autophagy in EA.hy926 cells and FOXO3 was identified as a target gene of miR-92a. Therefore, it was hypothesized that miR-92a may regulate the autophagic function of EA.hy926 cells by regulating the expression of FOXO3. To further verify this hypothesis, the effect of FOXO3 on the autophagy of EA.hy926 cells was studied. siFOXO3 was transfected into rapa-EA.hy926 cells to silence the FOXO3 gene, and the results showed that siFOXO3 significantly inhibited the autophagic activity of rapa-EA.hy926 cells. In addition, the miR-92a inhibitor and siFOXO3 were co-transfected into rapa-EA.hy926 cells to observe whether FOXO3 silencing could reverse the effects of the miR-92a inhibitor on autophagy in rapa-EA.hy926 cells. The results showed that knockdown of FOXO3 could reverse the promoting effect of the miR-92a inhibitor on the autophagic activity of rapa-EA.hy926 cells, further confirming that miR-92a may regulate the autophagic activity of EA.hy926 cells through targeted inhibition of FOXO3 expression.

The present study provided initial evidence to suggest that miR-92a may suppress the autophagic activity of EA.hy926 cells by inhibiting the expression of FOXO3. Therefore, it may be hypothesized that miR-92a not only induces EC apoptosis and inflammation (48,50) but also inhibits the autophagic activity of ECs by inhibiting FOXO3 expression, resulting in EC injury. Because of the significant role of impaired EC autophagic activity in the pathological processes of cardiovascular disease, miR-92a inhibitors may be used as EC protective factors that could provide a novel therapeutic approach for cardiovascular disease; however, one miRNA can regulate multiple target genes, and the signaling pathways of miRNAs regulating autophagy are extremely complex. Therefore, whether miR-92a also regulates EC autophagy by regulating the expression of other target genes or signaling pathways needs further study. In addition, the rapamycin-treated EA.hy926 cell line was an effective research model for *in vitro* experiments; however, it is necessary to perform experiments on animals to verify whether miR-92a influences autophagic activity via an identical mechanism in living organisms. With the in-depth study of miR-92a in cardiovascular diseases, the relationship between cardiovascular diseases and miR-92a will become clearer, a development that may provide innovative ideas for the clinical diagnosis and treatment of various cardiovascular diseases.

Acknowledgements

Not applicable.

Funding

This study was supported by the Natural Science Foundation of Heilongjiang Province (grant no. LH2022H028).

Availability of data and materials

The data generated in the present study may be requested from the corresponding author.

Authors' contributions

LH contributed to the experimental design, revised the paper, and guided and supervised the entire experimental process. WC performed the experiments and authored the paper. BZ, LG, XS and ZZ participated in the data analysis, and the literature review and collation. LH and BZ confirm the authenticity of all the raw data. All authors read and approved the final version of the manuscript.

Ethics approval and consent to participate

Not applicable.

Patient consent for publication

Not applicable.

Competing interests

The authors declare that they have no competing interests.

References

1. Little PJ, Askew CD, Xu S and Kamato D: Endothelial dysfunction and cardiovascular disease: History and analysis of the clinical utility of the relationship. Biomedicines 96: 699, 2021.
2. Lin X, Ouyang S, Zhi C, Li P, Tan X, Ma W, Yu J, Peng T, Chen X, Li L and Xie W: Focus on ferroptosis, pyroptosis, apoptosis and autophagy of vascular endothelial cells to the strategic targets for the treatment of atherosclerosis. Arch Biochem Biophys 715: 109098, 2022.
3. Zhao F, Satyanarayana G, Zhang Z, Zhao J, Ma XL and Wang Y: Endothelial autophagy in coronary microvascular dysfunction and cardiovascular disease. Cells 11: 2081, 2022.
4. Mameli E, Martello A and Caporali A: Autophagy at the interface of endothelial cell homeostasis and vascular disease. FEBS J 28911: 2976-2991, 2021.
5. Li A, Gao M, Liu B, Qin Y, Chen L, Liu H, Wu H and Gong G: Mitochondrial autophagy: Molecular mechanisms and implications for cardiovascular disease. Cell Death Dis 135: 444, 2022.
6. Zhou X, Yang J, Zhou M, Zhang Y, Liu Y, Hou P, Zeng X, Yi L and Mi M: Resveratrol attenuates endothelial oxidative injury by inducing autophagy via the activation of transcription factor EB. Nutr Metab (Lond) 16: 42, 2019.
7. Peng Z, Zhan H, Shao Y, Xiong Y, Zeng L, Zhang C, Liu Z, Huang Z, Su H and Yang Z: 13-methylberberine improves endothelial dysfunction by inhibiting NLRP3 inflammasome activation via autophagy induction in human umbilical vein endothelial cells. Chin Med 15: 8, 2020.
8. Zhang L, He J, Wang J, Liu J, Chen Z, Deng B, Wei L, Wu H, Liang B, Li H, *et al*: Knockout RAGE alleviates cardiac fibrosis through repressing endothelial-to-mesenchymal transition (EndMT) mediated by autophagy. Cell Death Dis 12: 470, 2021.
9. Niu C, Chen Z, Kim KT, Sun J, Xue M, Chen G, Li S, Shen Y, Zhu Z, Wang X, *et al*: Metformin alleviates hyperglycemia-induced endothelial impairment by downregulating autophagy via the Hedgehog pathway. Autophagy 15: 843-870, 2019.
10. Ren H, Dai R, Nik Nabi WN, Xi Z, Wang F and Xu H: Unveiling the dual role of autophagy in vascular remodelling and its related diseases. Biomed Pharmacother 168: 115643, 2023.
11. Zhao S, Wang H, Xu H, Tan Y, Zhang C, Zeng Q, Liu L and Qu S: Targeting the microRNAs in exosome: A potential therapeutic strategy for alleviation of diabetes-related cardiovascular complication. Pharmacol Res 173: 105868, 2021.
12. Wronska A: The role of microRNA in the development, diagnosis, and treatment of cardiovascular disease: Recent developments. J Pharmacol Exp Ther 3841: 123-132, 2023.
13. Wojciechowska A, Osiak A and Kozar-Kamińska K: MicroRNA in cardiovascular biology and disease. Adv Clin Exp Med 26: 868-874, 2017.
14. Doebele C, Bonauer A, Fischer A, Scholz A, Reiss Y, Urbich C, Hofmann WK, Zeiher AM and Dimmeler S: Members of the microRNA-17-92 cluster exhibit a cell-intrinsic antiangiogenic function in endothelial cells. Blood 115: 4944-4950, 2010.
15. Bonauer A, Carmona G, Iwasaki M, Mione M, Koyanagi M, Fischer A, Burchfield J, Fox H, Doebele C, Ohtani K, *et al*: MicroRNA-92a controls angiogenesis and functional recovery of ischemic tissues in mice. Science 324: 1710-1713, 2009.
16. Li M, Guan X, Sun Y, Mi J, Shu X, Liu F and Li C: miR-92a family and their target genes in tumorigenesis and metastasis. Exp Cell Res 323: 1-6, 2014.
17. Wu C, Huang RT, Kuo CH, Kumar S, Kim CW, Lin YC, Chen YJ, Birukova A, Birukov KG, Dulin NO, *et al*: Mechanosensitive PPAP2B regulates endothelial responses to atherorelevant hemodynamic forces. Circ Res 174: e41-e53, 2015.
18. Kumar S, Kim CW, Simmons RD and Jo H: Role of flow-sensitive microRNAs in endothelial dysfunction and atherosclerosis: Mechanosensitive athero-miRs. Arterioscler Thromb Vasc Biol 34: 2206-2216, 2014.
19. Zhang Y, Cheng J, Chen F, Wu C, Zhang J, Ren X, Pan Y, Nie B, Li Q and Li Y: Circulating endothelial microparticles and miR-92a in acute myocardial infarction. Biosci Rep 37: BSR20170047, 2017.
20. Carena MC, Badi I, Polkinghorne M, Akoumianakis I, Psarros C, Wahome E, Kotanidis CP, Akawi N, ntonopoulos AS, Chauhan J, *et al*: Role of human epicardial adipose tissue-derived miR-92a-3p in myocardial redox state. J Am Coll Cardiol 82: 317-332, 2023.
21. Liu Y, Li Q, Hosen MR, Zietzer A, Flender A, Levermann P, Schmitz T, Fruhwald D, Goody P, Nickenig G, *et al*: Atherosclerotic conditions promote the packaging of functional MicroRNA-92a-3p into endothelial microvesicles. Circ Res 124: 575-587, 2019.
22. Parahuleva MS, Lipps C, Parviz B, Holschermann H, Schieffer B, Schulz R and Euler G: MicroRNA expression profile of human advanced coronary atherosclerotic plaques. Sci Rep 8: 7823, 2018.
23. Wang H, Xie Y, Salvador AM, Zhang Z, Chen K, Li G and Xiao J: Exosomes: Multifaceted messengers in atherosclerosis. Curr Atheroscler Rep 22: 57, 2020.
24. Park CS, Kim I, Oh GC, Han JK, Yang HM, Park KW, Cho HJ, Kang HJ, Koo BK, Chung WY, *et al*: Diagnostic utility and pathogenic role of circulating MicroRNAs in vasospastic angina. J Clin Med 9: 1313, 2020.
25. Alexandru N, Constantin A, Nemecz M, Comarita IK, Vilcu A, Procopciuc A, Tanko G and Georgescu A: Hypertension associated with hyperlipidemia induced different MicroRNA expression profiles in plasma, platelets, and Platelet-derived microvesicles; Effects of endothelial progenitor cell therapy. Front Med (Lausanne) 6: 280, 2019.
26. Wang W, Li Z, Zheng Y, Yan M, Cui Y and Jiang J: Circulating microRNA-92a level predicts acute coronary syndrome in diabetic patients with coronary heart disease. Lipids Health Dis 18: 22, 2019.
27. Wiese CB, Zhong J, Xu ZQ, Zhang Y, Ramirez Solano MA, Zhu W, Linton MF, Sheng Q, Kon V and Vickers KC: Dual inhibition of endothelial miR-92a-3p and miR-489-3p reduces renal injury-associated atherosclerosis. Atherosclerosis 282: 121-131, 2019.
28. Shang F, Wang SC, Hsu CY, Miao Y, Martin M, Yin Y, Wu CC, Wang YT, Wu G, Chien S, *et al*: MicroRNA-92a Mediates endothelial dysfunction in CKD. J Am Soc Nephrol 2811: 3251-3261, 2017.
29. Livak KJ and Schmittgen TD: Analysis of relative gene expression data using real-time quantitative PCR and the 2(-Delta Delta C(T)) method. Methods 254: 402-408, 2001.
30. Yang P, Luo XL, Mo GJ, Tao XJ, Shen F and Ou HS: The effects of miR-24 on proliferation, metastasis, and autophagy of human umbilical vein endothelial cells. Shandong Med J 57: 24-27, 2017.
31. Feng Y, Yang H, Yue Y and Tian F: MicroRNAs and target genes in epileptogenesis. Epilepsia 61: 2086-2096, 2020.
32. Seok H, Ham J, Jang ES and Chi SW: MicroRNA target recognition: Insights from Transcriptome-Wide Non-canonical interactions. Mol Cells 39: 375-381, 2016.
33. Long J, Wang J, Dong Y, Yang J, Xie G and Tong Y: Prolyl isomerase Pin1 promotes autophagy and cancer cell viability through activating FoxO3 signalling. Cell Signal 113: 110940, 2024.
34. Liang L, Hui K, Hu C, Wen Y, Yang S, Zhu P, Wang L, Xia Y, Qiao Y, Sun W, *et al*: Autophagy inhibition potentiates the anti-angiogenic property of multikinase inhibitor anlotinib through JAK2/STAT3/VEGFA signaling in non-small cell lung cancer cells. J Exp Clin Cancer Res 381: 71, 2019.
35. Yang Z, Huang C, Wen X, Liu W, Huang X, Li Y, Zang J, Weng Z, Lu D, Tsang CK, *et al*: Circular RNA circ-FoxO3 attenuates blood-brain barrier damage by inducing autophagy during ischemia/reperfusion. Mol Ther 303: 1275-1287, 2022.
36. Zhang S, Tian W, Duan X, Zhang Q, Cao L, Liu C, Li G, Wang Z, Zhang J, Li J, *et al*: Melatonin attenuates diabetic cardiomyopathy by increasing autophagy of cardiomyocytes via regulation of VEGF-B/GRP78/PERK signaling pathway. Cardiovasc Diabetol 231: 19, 2024.
37. Zhou C, Shen L, Mao L, Wang B, Li Y and Yu H: miR-92a is upregulated in cervical cancer and promotes cell proliferation and invasion by targeting FBXW7. Biochem Biophys Res Commun 4581: 63-69, 2015.
38. Wang Y, Song X, Li Z, Liu N, Yan Y, Li T, Sun W, Guan Y, Li M, Yang Y, *et al*: MicroRNA-103 protects coronary artery endothelial cells against H_2O_2-Induced oxidative stress via BNIP3-mediated End-stage autophagy and antipyroptosis pathways. Oxid Med Cell Longev 2020: 8351342, 2020.
39. Xu Q, Meng S, Liu B, Li MQ, Li Y, Fang L and Li YG: MicroRNA-130a regulates autophagy of endothelial progenitor cells through Runx3. Clin Exp Pharmacol Physiol 41: 351-357, 2014.
40. Lu Z, Shen J, Chen X, Ruan Z, Cai W, Cai S, Li M, Yang Y, Mo J, Mo G, *et al*: Propofol upregulates MicroRNA-30b to inhibit excessive autophagy and apoptosis and attenuates Ischemia/Reperfusion injury in vitro and in patients. Oxid Med Cell Longev 2022: 2109891, 2022.
41. Wu D, Liang M, Dang H, Fang F, Xu F and Liu C: Hydrogen protects against hyperoxia-induced apoptosis in type II alveolar epithelial cells via activation of PI3K/Akt/Foxo3a signaling pathway. Biochem Biophys Res Commun 4952: 1620-1627, 2018.

42. Shi XY, Ding W, Li TQ, Zhang YX and Zhao SC: Histone deacetylase (HDAC) inhibitor, suberoylanilide hydroxamic Acid (SAHA), induces apoptosis in prostate cancer cell lines via the Akt/FOXO3a signaling pathway. Med Sci Monit 23: 5793-5802, 2017.
43. Hao W, Dian M, Zhou Y, Zhong Q, Pang W, Li Z, Zhao Y, Ma J, Lin X, Luo R, *et al*: Autophagy induction promoted by m6A reader YTHDF3 through translation upregulation of FOXO3 mRNA. Nat Commun 13, 5845: 2022.
44. Zhao C, Li X, Sun G, Liu P, Kong K, Chen X, Yang F and Wang X: CircFOXO3 protects against osteoarthritis by targeting its parental gene FOXO3 and activating PI3K/AKT-mediated autophagy. Cell Death Dis 13: 932, 2022.
45. Nho RS and Hergert P: FoxO3a and disease progression. World J Biol Chem 5: 346-354, 2014.
46. Sun L, Zhao M, Wang Y, Liu A, Lv M, Li Y, Yang X and Wu Z: Neuroprotective effects of miR-27a against traumatic brain injury via suppressing FoxO3a-mediated neuronal autophagy. Biochem Biophys Res Commun 482: 1141-1147, 2017.
47. Li F, Long TY, Bi SS, Sheikh SA and Zhang CL: circPAN3 exerts a profibrotic role via sponging miR-221 through FoxO3/ATG7-activated autophagy in a rat model of myocardial infarction. Life Sci 257: 118015, 2020.
48. Song L, Zhou F, Cheng L, Hu M, He Y, Zhang B, Liao D and Xu Z: MicroRNA-34a suppresses autophagy in alveolar type II epithelial cells in acute lung injury by inhibiting FoxO3 expression. Inflammation 40: 927-936, 2017.
49. Long C, Cen S, Zhong Z, Zhou C and Zhong G: FOXO3 is targeted by miR-223-3p and promotes osteogenic differentiation of bone marrow mesenchymal stem cells by enhancing autophagy. Hum Cell 34: 14-27, 2021.
50. Zhou Y, Wei W, Shen J, Lu L, Lu T, Wang H and Xue X: Alisol A 24-acetate protects oxygen-glucose deprivation-induced brain microvascular endothelial cells against apoptosis through miR-92a-3p inhibition by targeting the B-cell lymphoma-2 gene. Pharm Biol 59: 513-524, 2021.